An Alternative Design of a Compact and Portable Six-Port Reflectometer for 2.4 GHz Reflection Coefficient Measurements

G. Hernandez-Veliz, F. A. Uribe, *Senior Member IEEE,* and C. A. Bonilla-Barragán

***Abstract*—In this article, the design and implementation of a compact and portable six-port reflectometer for measuring the reflection coefficient at 2.4 GHz is presented. The proposed design utilizes reduced-size components, such as an RF generator and an acquisition board, achieving a portable solution that can be used outside the RF laboratory. In this design, the six-port circuit consists of only two microstrip directional couplers with an angularly equidistant distribution of their *q*-points. This configuration facilitates the implementation of the reflectometer, reducing complexity without sacrificing accuracy, even when compared to a commercial VNA. This design is an attractive and efficient alternative for research projects requiring the use of six-port reflectometry technique.**

Link to graphical and video abstracts, and to code: https://latamt.ieeer9.org/index.php/transactions/article/view/9302

***Index Terms*—six-port reflectometer, six-port circuit, reflection coefficient measurement, high frequency circuits**

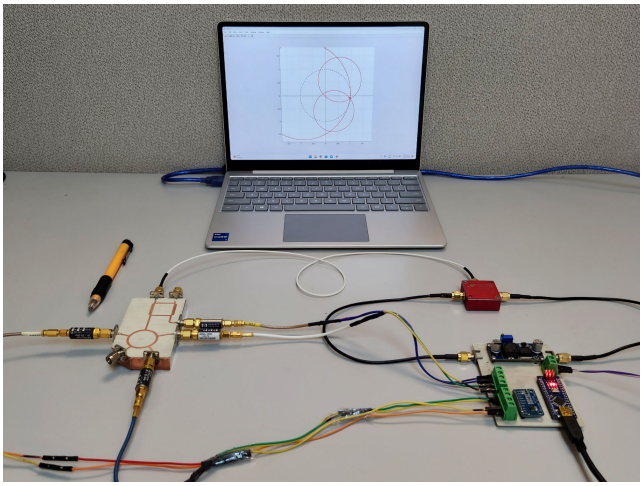

Fig. 1. Proposed six-port reflectometer.

I. Introducction

In this article, we propose the design of a six-port reflectometer (SPR) capable of measuring the reflection coefficient at 2.4 GHz. This design stands out for its simplicity and ease of replicability, thanks to its affordable and simple components, as shown in Fig. 1. The six-port circuit is composed of only two directional couplers, a VCO is used as the RF generator, and a specific DAQ board configuration, is presented for this purpose. In addition to providing the theoretical basis for the six-port circuit design, the calibration and implementation process are addressed in a graphical and intuitive manner. Despite its simplicity, the design maintains a measurement accuracy of over 90% compared to a commercial VNA.

Although some alternative proposals improve characteristics such as bandwidth [1], accuracy [2], and the elimination of matching networks at the diode ports [3], they do so at the expense of highly complex designs that require specialized methods for replicability. Some of these designs typically involve the fabrication of double-sided six-ports with multiple directional couplers and additional components [4], such as resistors integrated into the circuit. Therefore, the proposed design presents itself as an attractive alternative, especially for researchers from other disciplines, such as biomedical engineering or materials science, who can benefit from a reflectometer without having to face the complexity of the design and implementation of other configurations. This six-port reflectometer offers an accessible and efficient option for the implementation of the six-port reflectometry technique

The six-port reflectometer (SPR) is a measurement device commonly used as an alternative to commercial VNAs [5]. The SPR employs scalar power measurements in a passive network to determine the reflection coefficient of the DUT (Device Under Test) [6]. The six-port reflectometer offers several advantages over commercial VNAs, such as its high adaptability in situations where, due to cost and complexity, it is not feasible to modify or adapt commercial VNAs. This is especially true in research environments or for measuring experimental circuits [7]. As a result, six-port reflectometry has been implemented in various fields, such as material property monitoring [8], [9], [10], radar systems [11], [12], and biomedical applications [13], [14], [15], [16], among others.

With the SPR, the value of Γ_{DUT} is geometrically obtained through a mathematical model that generates three circles in the complex Γ plane [6]. The radii of these three circles depend on the constants of the six-port used and the power ratios measured at four ports of the six-port circuit. Consequently,

The associate editor coordinating the review of this manuscript and approving it for publication was Roberto S. Murphy (*Corresponding author: Gerardo Hernandez-Veliz*).

G. Hernandez-Veliz, F. A. Uribe, and C. A. Bonilla-Barragan are with Universidad de Guadalajara, Guadalajara, Mexico (e-mails: gerardo.hveliz@academicos.udg.mx, felipe.uribe@academicos.udg.mx, and alberto.bonilla@academicos.udg.mx).

the value of Γ_{DUT} is determined by trilateration, which means it takes its value based on the point in the plane where the three circles intersect. To reduce measurement uncertainty, various recommendations have been proposed, among which the need for the centers of the three circles or q-points, to be angularly equidistantly distributed in the plane stands out [17]. This represents one of the main challenges in developing an efficient six-port reflectometer.

II. Design and Setup

The diagram of the proposed six-port reflectometer design is shown in Fig. 2. It consists of a six-port circuit with two directional couplers, which is an alternative version to the six-port circuit design presented in [18], where a 90° hybrid coupler is used as a two-way directional coupler. In the design we propose for the six-port circuit, by using the 90° hybrid coupler as a two-way splitter, we reduce the complexity of the circuit and implement it in a single microstrip structure. This six-port network exhibits a theoretically angularly equidistant distribution in its q-points (centers), as shown in the port analysis performed in [19].

In this particular case, a six-port circuit, as proposed in [19], was implemented using a Rogers 4350B substrate with a relative permittivity ε_r of 3.6 and thickness h of 0.66mm, mounted on an aluminum plate and with copper tape to ensure the ground connection. This setup provided a more robust structure, allowing connectors to be mounted with enough stiffness to use a torque wrench on the circuit's ports, all without affecting the power distribution of the six-port circuit, as confirmed by characterizing its S-parameters. To estimate the error or verify its proper functioning, the simulated S-parameters were compared against the measured ones, showing consistency with the theoretical values from [19].

A 2.4 GHz VCO module is employed as the signal generator, controlled by a voltage module mounted on the same DAQ board, and it was previously calibrated with a spectrum analyzer to ensure the RF signal frequency at 2.4 GHz. In the six-port reflectometer technique, the precision of the RF signal source is not as critical because the reflection coefficient of the DUT is obtained through power ratios, and since the circuit's S parameters remain stable around the resonance frequency, there are no significant effects due to slight variations in the source's accuracy.

The power detectors must be capable of operating at the design frequency of the reflectometer, and their maximum detection power must be considered, as this value will determine the RF source power. For the proposed design, HP-8474C detectors are used. They have an operating frequency range of 0.01 to 33 GHz, with a sensitivity of 0.4 mW/ μW, a maximum detection power of 200 mW, and an impedance of 50 Ω. They operate by generating a DC (direct current) signal based on the amplitude of the received RF signal. A higher sensitivity in the diode's mW/ μW ratio will increase the accuracy of the reflectometer.

The data acquisition (DAQ) card is specifically designed for the reflectometer, comprising a 16-bit ADC ADS1115 with 4 channels and the capability to read negative voltages. These components, along with a development board, enable data acquisition to be sent via serial-USB for processing on the PC.

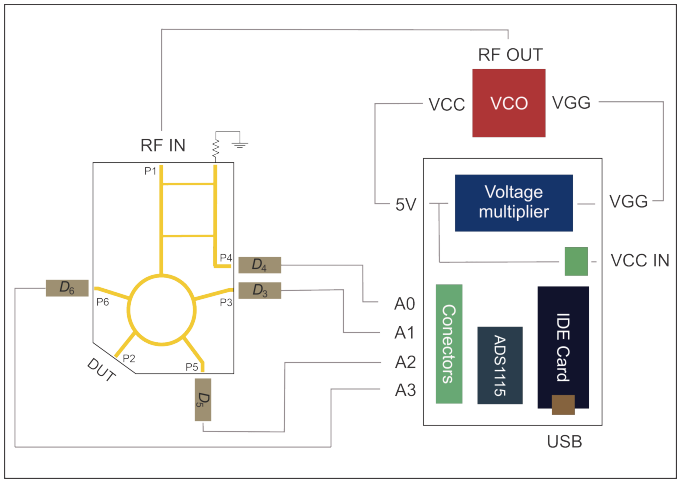

Fig. 2. Connection diagram of the elements comprising the proposed six-port reflectometer design. Where P1, P2, P3, P4, P5 and P6 are the Ports of ths Six-Port circuit. D_3, D_4, D_5 and D_6 are the power detector diodes. And A0, A1, A2 and A3 are the Ports of the ADC model ADS1115.

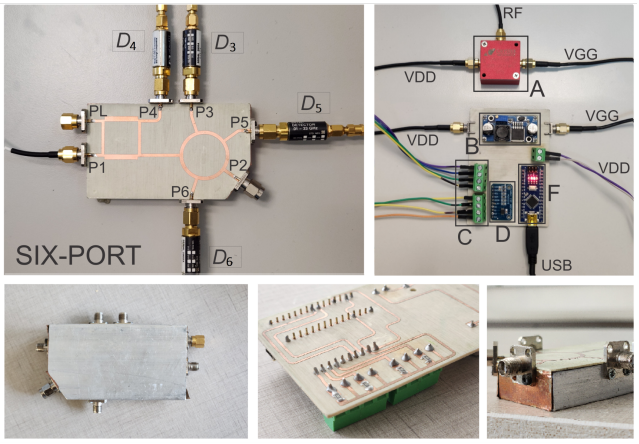

Fig. 3. Elements that make up the six-port reflectometer. The six-port circuit with Ports P1, P2, P3, P4, P5, P6 and PL. The diodes power detectors D_3, D_4, D_5 and D_6, the VCO (A), the module of voltaje control of the VCO (B), the diodes conectors to the ADC (C), the ADS1115 (D) and the IDE card (F).

These components are depicted in Fig. 3. It is worth mentioning that some elements that make up the proposed reflectometer can be replaced with components of similar characteristics or that meet the design requirements, such as the RF source, power detectors, and even the acquisition card, depending on the required accuracy and cost.

The data processing for measuring Γ_{DUT} is implemented using Matlab, based on the general equations of six-port reflectometry [6], as follows

$$|\Gamma_{\mathrm{DUT}} - q_3|^2 = \left|\frac{D}{A}\right|^2 \frac{P_3}{P_4}, \tag{1a}$$

$$|\Gamma_{\mathrm{DUT}} - q_5|^2 = \left|\frac{D}{E}\right|^2 \frac{P_5}{P_4}, \tag{1b}$$

$$|\Gamma_{\mathrm{DUT}} - q_6|^2 = \left|\frac{D}{G}\right|^2 \frac{P_6}{P_4}. \tag{1c}$$

In equations (1), q_3, q_5, and q_6 represents the location of the centers of the each circle in the plane. The variables P_i (where i = 1-4) are the voltages as a function of the powers measured by the four power detector. And the values D and N (where N = A, E, G, D) are constants dependent on the characteristics of the six-port circuit. Corresponding A for q_3, E for q_5, and G for q_6 respectively. These values are obtained through the analysis of the ports of the six-port circuit [19].

III. Calibration and Equations

The calibration of the reflectometer follows an alternative technique to that described in [20]. Four calibration standards (S_X, S_Y, S_Z, and Load) are employed, three of which are intended to represent ideally equidistantly spaced shifted shorts on the unit circle. In this calibration, we use the same short standard from a commercial SOLT calibration kit as three distinct standards (S_X, S_Y and S_Z). To achieve the necessary phase shifts, a different length of transmission line is added between the measurement port and the short standard for each standard, creating the desired angular separation for accurate calibration. This achieves three angularly equidistant points on the unit circle, that is, three equally spaced offset shorts, which must be previously verified with a VNA, and their respective reflection coefficients characterized at the desired frequency, which in this case is 2.4 GHz. This is necessary because the further they deviate from an equidistant distribution, the greater the calibration uncertainty and, consequently, the accuracy of the reflectometer. Finally, the fourth calibration standard is a 50 Ω standard (L).

Thus, the reflectometer calibration involves obtaining three calibration constants B_3, B_5 and B_6 and three calibrated q-points Q_3, Q_5 and Q_6.

With this process, differences between the theoretical model of the six-port circuit and the physical characteristics of the constructed circuit are compensated for. The lengths of the tracks of each port are characterized, and parasitic effects such as noise caused by connectors, soldering, and non-ideal couplings between the six-port circuit and other elements like the generator and power detector are compensated for.

The calibration begins with the measurement of each of the standards, obtaining four voltage vectors, each with four voltage values, resulting in a total of 16 values. These values are generated from the power readings of the four detectors in each calibration measurement. The values can be organized into a table, as shown in Table I.

Each vector (row) corresponds to the measurements taken for each of the standards, and each value represents the voltage as a function of the power measured P_4, P_3, P_5 and P_6 by each power detector diode D_4, D_3, D_5 and D_6, according to the incident power at its respective port. After performing the measurements on the calibration standards, the calibration constants B_3, B_5 and B_6 are obtained

TABLE I
Voltage Vector Values, as a Function of the Power Measured During Calibration

	P_4	P_3	P_5	P_6
Standard S_X	X_4	X_3	X_5	X_6
Standard S_Y	Y_4	Y_3	Y_5	Y_6
Standard S_Z	Z_4	Z_3	Z_5	Z_6
Standard Load	L_4	L_3	L_5	L_6

$$B_3 = 1 - \frac{L_3}{L_4}, \quad B_5 = 1 - \frac{L_5}{L_4}, \quad \text{y} \quad B_6 = 1 - \frac{L_6}{L_4}. \tag{2}$$

Subsequently, similar to how the value of Γ_{DUT} is determined through trilateration, the locations of the three calibrated q-points (or Q-points) are determined in the same way, necessary for the final equations of the reflectometer, i.e., one Q point per plane.

To generate the calibration planes D_3, D_5 and D_6, three circles per plane need to be generated, where the centers of these circles are the same in all three planes, being the impedances at 2.4 GHz of the calibration standards S_X, S_Y, and S_Z. Meanwhile, the radii take their value based on the constants of the six-port circuit and the power relationships obtained during the measurement of the calibration standards. The constants of the six-port structure D, A, E, and G take their numerical value based on the port analysis of the six-port circuit [19]. The equations of the circles to obtain the Q_3, Q_5 and Q_6 points through the planes D_3, D_5 and D_6.

To obtain the point Q_3 in the plane D_3, it is achieved by the intersection of the three circles whose equations are

$$|Q_3 - S_X|^2 = 4\frac{X_3(B_3)}{X_4}, \tag{3a}$$

$$|Q_3 - S_Y|^2 = 4\frac{Y_3(B_3)}{Y_4}, \tag{3b}$$

$$|Q_3 - S_Z|^2 = 4\frac{Z_3(B_3)}{Z_4}. \tag{3c}$$

The equations to obtain the point Q_5 in the plane D_5 are obtained by the intersection of the three circles described by

$$|Q_5 - S_X|^2 = 4\frac{X_5(B_5)}{X_4}, \tag{4a}$$

$$|Q_5 - S_Y|^2 = 4\frac{Y_5(B_5)}{Y_4}, \tag{4b}$$

$$|Q_5 - S_Z|^2 = 4\frac{Z_5(B_5)}{Z_4}. \tag{4c}$$

The equations describing the circles to find the point Q_6 in the plane D_6 are expressed as

$$|Q_6 - S_X|^2 = 4\frac{X_6(B_6)}{X_4}, \tag{5a}$$

$$|Q_6 - S_Y|^2 = 4\frac{Y_6(B_6)}{Y_4}, \tag{5b}$$

$$|Q_6 - S_Z|^2 = 4\frac{Z_6(B_6)}{Z_4}. \tag{5c}$$

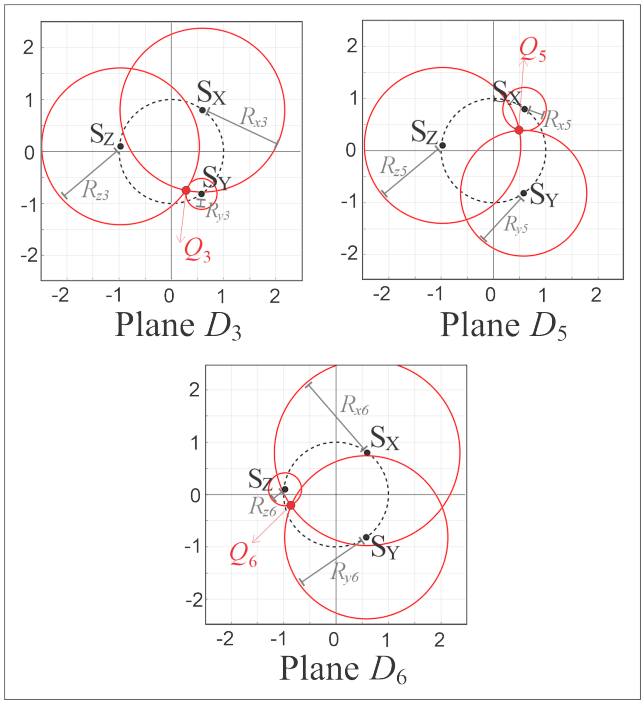

Fig. 4. Example of obtaining the points Qi through the planes Di.

Since the equations of the circles solving the calibration are presented in the same form as the equations of the general reflectometry model, that is, as $(x-h)^2+(y-k)^2=r^2$, the values of the radii of the calibration circles (to the right of the equal sign) can be organized in a table II, according to equations 3 - 5.

With this, we obtain a table in which the rows contain the radii generated with the values obtained using the same calibration standard. The columns, on the other hand, represent the radii generated by the same power detector. And each column also corresponds to a different plane, as shown in Table II.

TABLE II
RADII FOR THE CALIBRATION PLANES D_i

	D_3 Plane	D_5 Plane	D_6 Plane
Radii S_X	R_{x3}	R_{x5}	R_{x6}
Radii S_Y	R_{y3}	R_{y5}	R_{y6}
Radii S_Z	R_{z3}	R_{z5}	R_{z6}

With all the previous data, we can generate the planes to obtain the calibrated q-points or also called Q-points. Remembering that the centers of the circles of the three planes are defined by the values of the impedances of the calibration standards S_X, S_Y, and S_Z. This process is shown in the plots of Fig. 4.

Finally, we obtain the equations to determine the value of Γ_{DUT} (Γ_2) with the proposed reflectometer design. These equations are presented in the form

$$|\Gamma_{DUT}-Qi|^2=\left|\frac{D}{N_i}\right|^2\frac{P_i(B_i)}{P_4}. \tag{6}$$

Where Q_i (to i = 3, 5 and 6) represents the center of each circle in the complex plane Γ. The expression $\left|\frac{D}{N_i}\right|^2$ takes its value based on the constants dependent on the characteristics of the six-port circuit (where $N_i = A, E$, and G). And, as a whole, the expression $|D/N_i;|^2\,(Pi\,(B_3)/P_4)$ defines the value of the radius of each circle. All this in terms of the impedance presented at Port P2 (DUT) of the six-port circuit.

Therefore, the developed equations describing the three circles necessary to solve Γ_{DUT}, taking into account the reflectometer calibration and the characteristics of the six-port circuit, are expressed as

$$|\Gamma_{DUT}-Q_3|^2=(4)\frac{P_3(B_3)}{P_4}, \tag{7a}$$

$$|\Gamma_{DUT}-Q_5|^2=(4)\frac{P_5(B_5)}{P_4}, \tag{7b}$$

$$|\Gamma_{DUT}-Q_6|^2=(4)\frac{P_6(B_6)}{P_4}. \tag{7c}$$

Once the calibration constants have been resolved, it is sufficient to measure the powers P_4, P_3, P_5 and P_6, with the power detectors D_4, D_3, D_5 and D_6 to generate the three circles in the complex plane and define the value of Γ_{DUT} by intersecting the three circles in the complex plane Γ.

IV. TEST AND POSSIBILITIES

Once the calibration is done and the equations are implemented in the software, measurements were taken at 2.4 GHz with different test loads. For the test, various loads with different impedances were used, such as SMA loads, microstrip transmission line segments with SMA connectors, antennas, among others, regardless of their impedance or operating frequency, as the objective was simply to have an arbitrary element to evaluate its reflection directly at the measurement port of the six-port reflectometer. Subsequently, the same loads were measured with a commercial VNA to compare the results between both measurement devices. One of the measurements taken is presented in Fig. 5, where the measurement of Γ_{DUT} is shown using both devices, the six-port reflectometer and a commercial VNA (Agilent N5227A).

When evaluating the results, it is essential to consider that six-port reflectometry employs trilateration, while the commercial VNA uses the heterodyning technique. These differences are also reflected in the presentation of the results [21]. For this reflectometer, a code is used that implements an iterative method. It starts with an initial estimate of the point and progressively adjusts its position based on the differences between the distances calculated from the point to the centers of the circles and their respective radii. The process is repeated until the differences are small enough, within a defined tolerance, or a maximum number of iterations is reached. This approach does not require user intervention and can handle situations where the circles overlap or do not intersect perfectly. The estimated location of the Γ_{DUT} is displayed both numerically and graphically on the plane.

It is important to note that for this type of measurement (S-parameters or reflection coefficient), it is not necessary to

use an anechoic chamber, as this measurement evaluates the amount of reflected energy at the device's input port, without requiring free-field or radiation conditions in open space. In this case, the measurement is performed in the near field, where environmental interference is minimal and can be easily controlled.

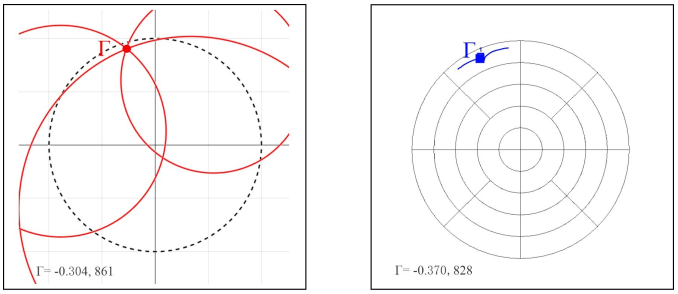

Fig. 5. Same DUT measured at 2.4 GHz with the (a) Six-Port Reflectometer and a (b) Vector Network Analyzer Agilent N5227A in polar format.

The various measurements taken with both devices are shown in the graph in Fig. 6, which graphically illustrates the differences in the results obtained by both devices. The values are shown in Table III.

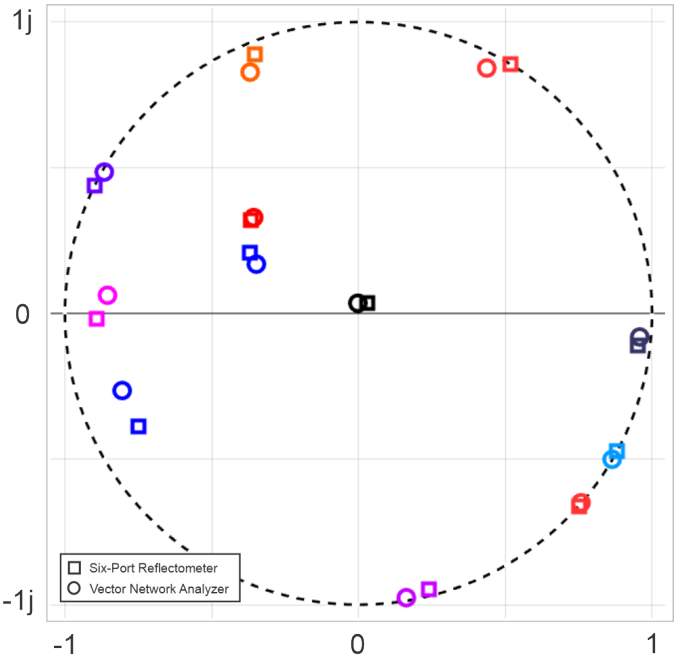

Fig. 6. Comparison of various DUT at 2.4 GHz with the Six-Port Reflectometer and a Vector Network Analyzer (Agilent N5227A) in polar format.

Upon observing the measurements, it was found that the proposed reflectometer presents an average difference in magnitude of 0.0366. In terms of phase, the average difference was 3.08°. These differences translate to a relative accuracy of 95.24% in magnitude and 92.93% in phase for the SPR compared to the commercial VNA (Agilent N5227A). While this value indicates a deviation that may be significant, it is essential to consider the significant difference in complexity and costs between both devices, which, when evaluating all these characteristics, yield highly attractive results.

TABLE III
MEASUREMENTS OBTAINED USING BOTH THE PROPOSED SIX-PORT REFLECTOMETER AND THE COMMERCIAL VNA

DUT	SPR	VNA	Difference
DUT 1	$0.074 \angle 126.25°$	$0.033 \angle 127.56°$	$0.041 \angle 1.31°$
DUT 2	$0.627 \angle 127.87°$	$0.485 \angle 137.33°$	$0.142 \angle 9.46°$
DUT 3	$0.921 \angle 172.76°$	$0.843 \angle 171.19°$	$0.079 \angle 1.57°$
DUT 4	$0.941 \angle -159.98°$	$0.943 \angle -174.09°$	$0.002 \angle 14.11°$
DUT 5	$0.598 \angle 134.66°$	$0.387 \angle 153.96°$	$0.211 \angle 19.30°$
DUT 6	$0.103 \angle 119.05°$	$0.050 \angle 124.33°$	$0.053 \angle 5.28°$
DUT 7	$0.996 \angle -109.96°$	$0.999 \angle -70.04°$	$0.003 \angle 39.92°$
DUT 8	$0.924 \angle -151.71°$	$0.898 \angle -167.26°$	$0.026 \angle 15.55°$
DUT 9	$0.913 \angle 109.44°$	$0.907 \angle 114.07°$	$0.006 \angle 4.63°$
DUT 10	$1.000 \angle -6.65°$	$0.961 \angle -4.83°$	$0.039 \angle 1.82°$
DUT 11	$0.942 \angle -151.17°$	$0.993 \angle -160.47°$	$0.051 \angle 9.30°$
DUT 12	$0.976 \angle -86.59°$	$0.990 \angle -80.58°$	$0.014 \angle 6.01°$
DUT 13	$0.987 \angle 61.90°$	$0.949 \angle 62.57°$	$0.038 \angle 0.67°$
DUT 14	$1.000 \angle -40.86°$	$0.990 \angle -40.61°$	$0.010 \angle 0.25°$
DUT 15	$0.981 \angle -28.83°$	$0.990 \angle -30.10°$	$0.009 \angle 1.27°$
DUT 16	$1.000 \angle 149.76°$	$0.980 \angle 152.12°$	$0.020 \angle 2.36°$

However, at some intersection points, significantly larger regions of discrepancy were observed compared to others, especially in areas near the center of the plane and corresponding to the better-coupled loads. This phenomenon was caused by the calibration used, which, in this particular case, compensates more intensely for the equipment errors in that region of the plane. Nevertheless, the iterative method performed very effectively in estimating the intersection point and determining a specific point on the plane.

One of the factors that has contributed to obtaining a region with greater uncertainty near the center of the complex plane is identified as the lack of linearity and precision of the ADC. In the specific model we have used for this configuration, it has been observed that the precision and linearity of the ADC are not optimal, which has led to the aforementioned phenomena. Linearity is a highly desirable characteristic in an analog-to-digital converter (ADC) because it ensures the accuracy of analog-to-digital signal conversions and maintains a constant relationship between the input signal and the digital output across the entire input range. However, while no ADC is perfectly linear in practice, better results can be obtained by using a higher-quality ADC, particularly one with better linearity. This specific model was used for reasons of size and cost.

It is worth mentioning that although some interesting designs of compact and portable six-port reflectometers have been proposed [13], [22], [23], some of them are designed for a specific application of the technique. This is in contrast to the proposed design, which can be used directly as an alternative to the commercial VNA but at a single specific frequency.

Nevertheless, despite the observed differences, the proposed reflectometer is considered an attractive alternative because it can offer sufficient accuracy for various applications, even though this design was primarily developed for measuring circuits and components at 2.4 GHz, primarily antennas. Addi-

tionally, it offers an excellent balance between simplicity, cost, and the benefits of its design by using low-cost components and materials, making it accessible and ideal for use in development and research stages. Furthermore, its compact and portable design facilitates the implementation of the technique in environments outside the RF laboratory.

Some functions of the proposed reflectometer design could improve if further studied and analyzed. For example, the bandwidth can be enhanced by optimizing the six-port circuit design, which is the main limiting factor. In that case, the *S*-parameters should be kept constant over a broader frequency range, particularly the S_{11} parameter, providing very good coupling within the desired frequency spectrum. Furthermore, to enable frequency sweeping, one must first ensure a wide bandwidth and then have a programmable RF signal source, which should be synchronized with the data acquisition card to measure the reflection coefficient across the desired frequency range

V. Conclusion

In this article, the design of a six-port reflectometer has been proposed, which stands out for its simplicity and ease of replicability due to its affordable and straightforward components. This device has proven to be a viable and accessible alternative to commercial VNAs for measuring Γ_{DUT} at 2.4 GHz. Through various tests and comparisons, it was determined that the six-port reflectometer exhibits a relative accuracy of 95.24% in magnitude and 92.93% in phase compared to a commercial VNA, which is notable considering the differences in complexity and cost between both devices.

Furthermore, the compact and portable design of the proposed reflectometer, along with its ease of implementation, makes it ideal for applications in development and research stages outside the traditional RF laboratory. In terms of practical application, the six-port reflectometer offers an accessible and effective solution for implementing six-port reflectometry technique in other areas of research, such as biomedicine and materials engineering, thus fostering innovation and experimentation in the field of microwave technology and opening the door to new applications in diverse and resource-limited contexts.

Clearly, the reflectometer presented here still has room for improvement, such as its bandwidth or the ability to perform frequency sweeps. However, due to its aforementioned advantages, it remains an excellent option, even as an alternative to commercial VNAs.

References

[1] A. Hassan, O. Abbas, “Design of a wide band six port reflectometer using broadside coupled lines,” Microwave and optical technology letters, 2018, vol. 60, Issue 9, pp. 2101-2103, https://doi.org/10.1002/mop.31310.

[2] K. Staszek, S. Gruszczynski and K. Wincza, “Six-Port Reflectometer Providing Enhanced Power Distribution,” IEEE Transactions on Microwave Theory and Techniques, vol. 64, no. 3, pp. 939-951, March 2016, 10.1109/TMTT.2016.2518681.

[3] K. Staszek, “Balanced six-port reflectometer with nonmatched power detectors,” IEEE Trans. Microw. Theory Techn., vol. 69, no. 11, pp. 4869–4878, Nov. 2021, 10.1109/TMTT.2021.3101701.

[4] J. J. Yao and S. P. Yeo, “Six-Port Reflectometer Based on Modified Hybrid Couplers,” IEEE Transactions on Microwave Theory and Techniques, vol. 56, no. 2, pp. 493-498, Feb. 2008, 10.1109/TMTT.2007.914626.

[5] C. A. Hoer, ”A Network Analyzer Incorporating Two Six-Port Reflectometers,” in IEEE Transactions on Microwave Theory and Techniques, vol. 25, no. 12, pp. 1070-1074, Dec. 1977, 10.1109/TMTT.1977.1129276.

[6] G. F. Engen, ”The Six-Port Reflectometer: An Alternative Network Analyzer,” IEEE Transactions on Microwave Theory and Techniques. vol. 25, no. 12, pp. 1075-1080, Dec. 1977, 10.1109/TMTT.1977.1129277.

[7] J. Martínez Moreno, A. S. Medina Vázquez, C. A. Bonilla Barragán, J. M. Villegas González and J. C. Aldaz Rosas, ”Radio Frequency Energy Harvesting System Making Use of 180° Hybrid Couplers and Multiple Antennas to Improve the DC Output Voltage,” in IEEE Latin America Transactions, vol. 18, no. 03, pp. 604-612, March 2020, 10.1109/TLA.2020.9082733.

[8] K. Kim, N. Kim, S. -H. Hwang, Y. -K. Kim and Y. Kwon, ”A Miniaturized Broadband Multi-State Reflectometer Integrated on a Silicon MEMS Probe for Complex Permittivity Measurement of Biological Material,” in IEEE Transactions on Microwave Theory and Techniques, vol. 61, no. 5, pp. 2205-2214, May 2013, 10.1109/TMTT.2013.2250992.

[9] K. Staszek, I. Piekarz, J. Sorocki, S. Koryciak, K. Wincza and S. Gruszczynski, ”Low-Cost Microwave Vector System for Liquid Properties Monitoring,” in IEEE Transactions on Industrial Electronics, vol. 65, no. 2, pp. 1665-1674, Feb. 2018, 10.1109/TIE.2017.2733423.

[10] S. Somwong, P. Wounchoum, M. Chongcheawchamnan, “Contamination detection in fresh natural rubber latex by a dry rubber content measurement system using microwave reflectometer,” Biosystems Engineering, 2017, vol. 164, pp. 181-188, https://doi.org/10.1016/j.biosystemseng.2017.10.013.

[11] F. Barbon, G. Vinci, S. Lindner, R. Weigel and A. Koelpin, ”A six-port interferometer based micrometer-accuracy displacement and vibration measurement radar,” 2012 IEEE/MTT-S International Microwave Symposium Digest, Montreal, QC, Canada, 2012, 10.1109/MWSYM.2012.6259624.

[12] S. Linz, F. Lurz, R. Weigel and A. Koelpin, ”Squircle-Based Calibration Algorithm for Six-Port Radar,” in IEEE Transactions on Microwave Theory and Techniques, vol. 67, no. 10, pp. 4023-4030, Oct. 2019, 10.1109/TMTT.2019.2931968.

[13] S. Julrat and S. Trabelsi, ”Portable Six-Port Reflectometer for Determining Moisture Content of Biomass Material,” in IEEE Sensors Journal, vol. 17, no. 15, pp. 4814-4819, 1 Aug.1, 2017, 10.1109/JSEN.2017.2718659.

[14] K. Kim, N. Kim, S. -H. Hwang, Y. -K. Kim and Y. Kwon, ”A Miniaturized Broadband Multi-State Reflectometer Integrated on a Silicon MEMS Probe for Complex Permittivity Measurement of Biological Material,” in IEEE Transactions on Microwave Theory and Techniques, vol. 61, no. 5, pp. 2205-2214, May 2013, 10.1109/TMTT.2013.2250992.

[15] G. Vinci et al., ”Six-Port Radar Sensor for Remote Respiration Rate and Heartbeat Vital-Sign Monitoring,” in IEEE Transactions on Microwave Theory and Techniques, vol. 61, no. 5, pp. 2093-2100, May 2013, 10.1109/TMTT.2013.2247055.

[16] S. Julrat and S. Trabelsi, ”Portable Six-Port Reflectometer for Determining Moisture Content of Biomass Material,” in IEEE Sensors Journal, vol. 17, no. 15, pp. 4814-4819, 1 Aug.1, 2017, 10.1109/JSEN.2017.2718659.

[17] Kamil Staszek, ”Investigation on Optimum Parameters of Six-Port Reflectometers,” International Journal of Information and Electronics Engineering vol. 9, no. 1, pp. 30-33, 2019, 10.18178/IJIEE.2019.9.1.700.

[18] G. P. Riblet and E. R. B. Hansson, ”The Use of a Matched Symmetrical Five-Port Junction to Make Six-Port Measurements,” 1981 IEEE MTT-S International Microwave Symposium Digest, Los Angeles, CA, USA, 1981, pp. 151-153, 10.1109/MWSYM.1981.1129852.

[19] G. Hernández Veliz, C. A. Bonilla Barragán, and F. A. Uribe Campos, “An Efficient 2.4 GHz Six-port Circuit Design to implement a Reflectometer”, IEEE Lat Am T, vol. 21, no. 7, pp. 858–865, Jul. 2023, 10.1109/TLA.2023.10244184.

[20] L. Qiao and S. P. Yeo, “Improved implementation of four-standard procedure for calibrating six-port reflectometers,” in IEEE Transactions on Instrumentation and Measurement, vol. 44, no. 3, pp. 632-636, June 1995, 10.1109/19.387297.

[21] K. Staszek, S. Gruszczynski and K. Wincza, ”Theoretical Limits and Accuracy Improvement of Reflection-Coefficient Measurements in Six-Port Reflectometers,” in IEEE Transactions on Microwave Theory and Techniques, vol. 61, no. 8, pp. 2966-2974, Aug. 2013, 10.1109/TMTT.2013.2269053.

[22] S. Somwong and M. Chongcheawchamnan, "A Portable System for Rapid Measurement of Dry Rubber Content With Contaminant Detection Feature," in IEEE Sensors Journal, vol. 18, no. 20, pp. 8329-8337, 15 Oct.15, 2018, 10.1109/JSEN.2018.2865478.
[23] Z. Peng and C. Li, "A portable 24-GHz FMCW radar based on six-port for short-range human tracking," 2015 IEEE MTT-S 2015 International Microwave Workshop Series on RF and Wireless Technologies for Biomedical and Healthcare Applications (IMWS-BIO), Taipei, Taiwan, 2015, pp. 81-82, 10.1109/IMWS-BIO.2015.7303787.

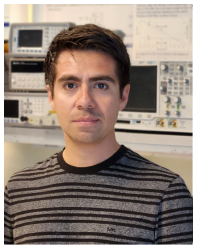

Gerardo Hernández Veliz is a communications and electronics engineer. He received his Ph.D. in Electronic Engineering from Universidad de Guadalajara in 2024. He currently serves as a professor in the Department of Electro-Photonics Engineering at CUCEI, Universidad de Guadalajara, Guadalajara México. His research interests include PCB design and printing, antenna design, microstrip circuits, high-frequency signal analysis, optoelectronics, and semiconductor physics.

Felipe A. Uribe (Senior Member, IEEE) received the M.Sc. degrees in electrical engineering from the University of Guadalajara, Guadalajara, México, in 1998 and the Ph.D. degree in electrical engineering from the Center for Research and Advanced Studies, Guadalajara, México, in 2002. From 2003 to 2006, he was a Full Professor with the Electrical Graduate Program, Autonomous University of Nuevo Leon, San Nicolás de los Garza, Mexico. In May 2006, he joined the Electrical Engineering Graduate Program, University of Guadalajara, where he is currently a full-time Researcher. His primary interests include the signal and image processing techniques for harmonic and transient analysis of smart grids.

Carlos Alberto Bonilla Barragán was born in Guadalajara, Jalisco, México, on September 5th, 1965. He received the B.Sc. degree in electronic and communications engineering and the MSc degree in Electronic Engineering with specialization in high frecuencies from the Universidad de Guadalajara, Jalisco, México, in 1992 and 2005 respectively. In 2013 he obtains his PhD in Sciences with the specialty of Electrical Engineering in High frequencies, degree obtained in the Universidad Autónoma de Baja California (UABC) in Méxicali. From 1994 is working as a teacher in the Universidad de Guadalajara. His areas of interest are the Design of Microwave Circuits and Antennas, Six-port reflectometers, and RF Harvesting circuits.